New Experiments on Convective Heat Loss

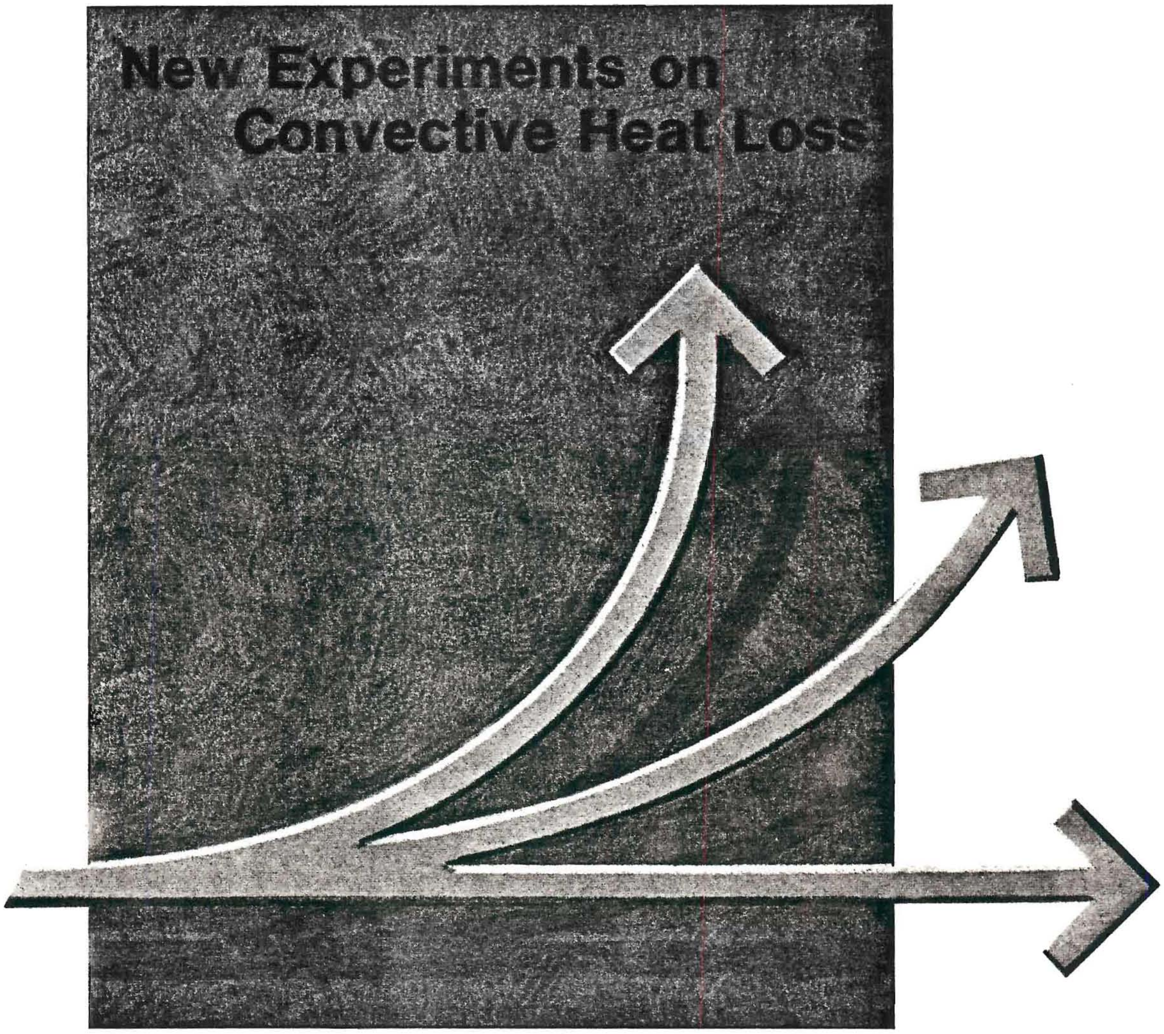

An understanding of convective heat loss is essential to the design of efficient solar central receivers.

In solar central-receiver systems, an array of heliostats reflects sunlight onto a receiver atop a tower. The receiver absorbs solar energy and uses it to heat a working fluid, which can be air, water, molten salt, or liquid metal. This heated fluid is used to provide process heat or to generate electric power in a thermal power plant (Figure 1).

The receiver's efficiency in absorbing and transferring solar energy to the working fluid is critical to the central-receiver concept since plant performance, capital cost, and, ultimately, the cost of energy produced are significantly affected by the receiver's efficiency. In addition to these economic ramifications, errors in estimates of energy loss entail the risk of perpetuating inefficient receiver designs and implanting incorrect receiver technology for the future.

To calculate receiver efficiency, predictions are required for energy losses from:

- Reflection of incoming solar energy
- Radiation from heated surfaces
- Heat conduction into the structure that supports the receiver and
- Convection (natural, forced, or mixed).

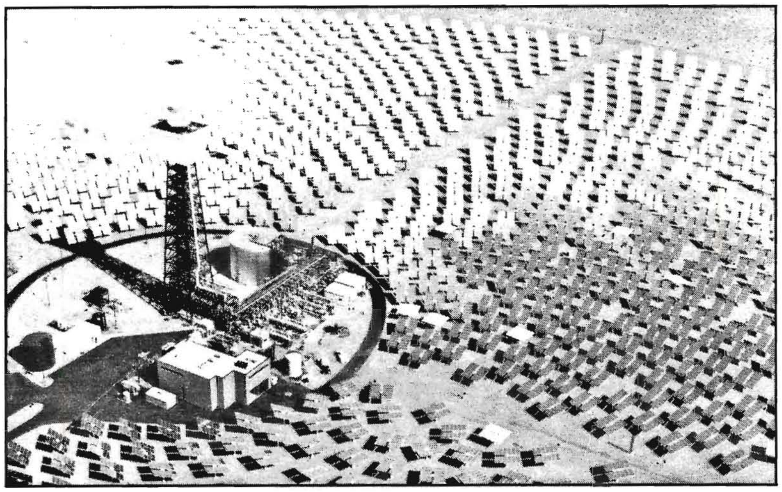

Figure 1.
Solar One, the 10-MW_e Solar Thermal Central Receiver Pilot Plant near Barstow, CA, is the world's largest solar electric generating station. It is designed to produce 10 MW_e of electric power for the Southern California Edison Company utility grid (after supplying the plant's own power requirements) for 8 hours on a clear summer-solstice day. The flat-plate experiment described in this article was designed to obtain information on the convective heat transfer that occurs on external-type receivers of the kind used in Solar One.

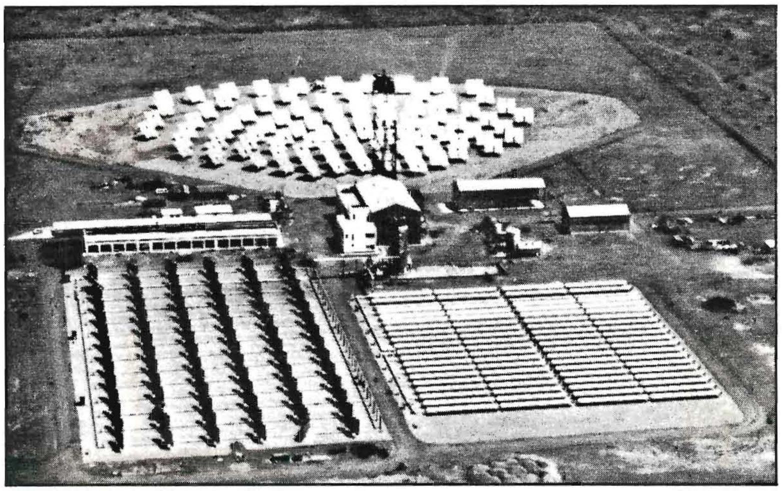

Located near Almería, Spain, the International Energy Agency's Small Solar Power Systems Project is designed to test two types of solar-thermal power plants. Our cavity experiment yielded information on convective heat transfer typical of the cavity-type receiver used in this plant. The facility was designed to produce 500 kW_e of electric power for 8 hours under the best weather conditions.

Figure 2 is a schematic of the receiver energy balance.

While methods exist for estimating the first three loss mechanisms, information needed to estimate convective heat losses has been, until recently, almost nonexistent. The large sizes, high surface temperatures, and complex geometries of central receivers have placed them in convective heat-transfer regimes for which there has been a dearth of experimental data and predictive methods.

Because of this lack of information, in 1979 we initiated the Central Receiver Convective Energy Loss Program, a research effort to establish a convective heat-loss data base, involving a number of universities and private firms. As part of the program, we were directly involved in two large-scale heat-transfer experiments: A flat-plate experiment to obtain information for external-type receivers such as the Solar Thermal Central Receiver Pilot Plant (Solar One) at Barstow, CA, and an experiment covering cavity-type receivers like the International Energy Agency's Small Solar Power Systems Project near Almeria, Spain.

Since scaling is difficult, we conducted the experiments "near-full-scale" and at temperatures that closely simulated actual receiver operating conditions. Despite the large sizes, high power requirements (up to 525 kW), and high temperatures involved, we conducted the experiments in a controlled, laboratory-type environment.

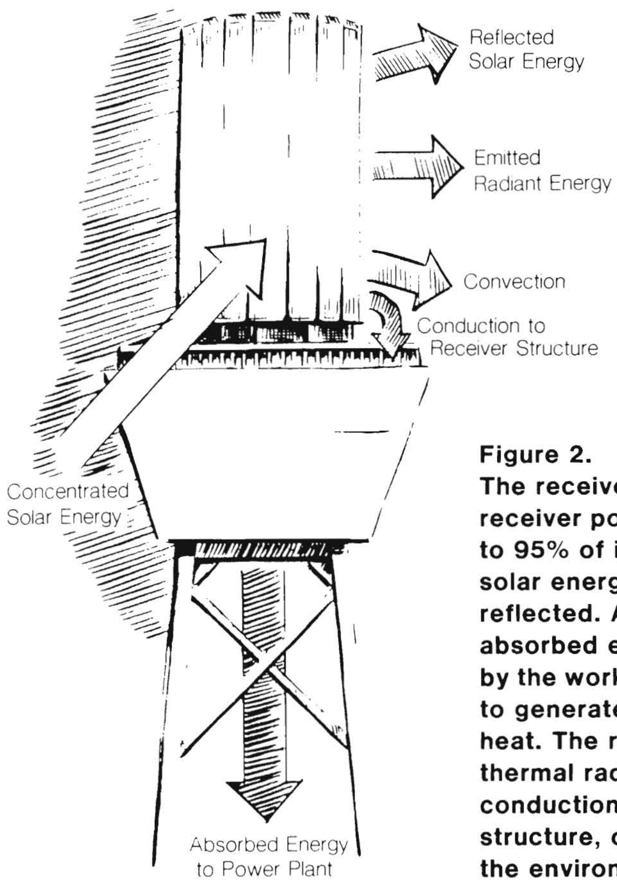

Figure 2.
The receiver of a solar central-receiver power plant absorbs 90% to 95% of incoming concentrated solar energy; the remainder is reflected. A large portion of the absorbed energy is carried away by the working fluid in the receiver to generate power or process heat. The rest is re-emitted as thermal radiation, lost by conduction to the receiver structure, or lost by convection to the environment.

Vertical Flat Plate Experiment

Convective heat transfer from external receivers can occur either in a forced-convection mode (wind-driven), a natural-convection mode (buoyancy-driven), or a combined forced and natural-convection mode (mixed convection). In addition, the surface temperature of a receiver is high in relation to ambient air temperature, so property variations in the air near the receiver surface resulting from large temperature gradients have significant effects on the convective heat-transfer process. We designed this experiment to obtain information primarily on mixed-convection heat transfer and the effects of property variations on both mixed and natural-convection heat transfer for regions of boundary-layer flow on external receivers.

The experimental apparatus consists of a large (3 m x 3 m), electrically heated, vertical flat plate placed parallel to the horizontal flow of air in a wind tunnel (Figure 3a).

Figure 3.
We conducted two large heat-transfer experiments, one on a large flat plate (a) and the other on a cubical cavity (b).

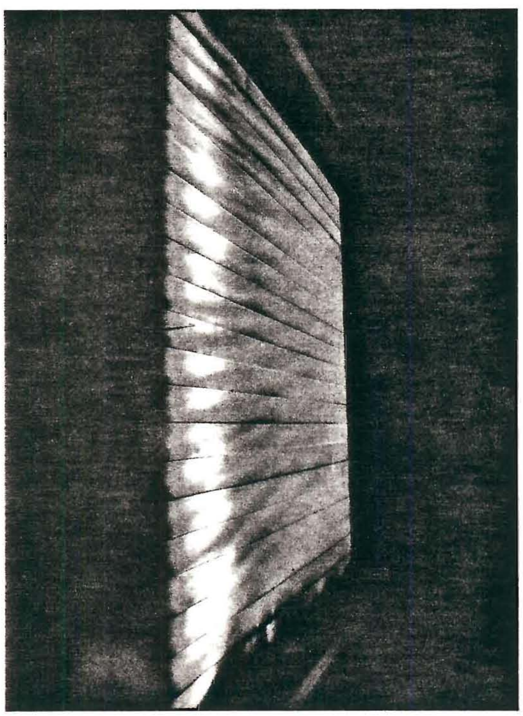

Size:	**3 m x 3 m**
Surface Temp:	**60°C to 650°C**
Wind Velocities	**0-6 m/s**

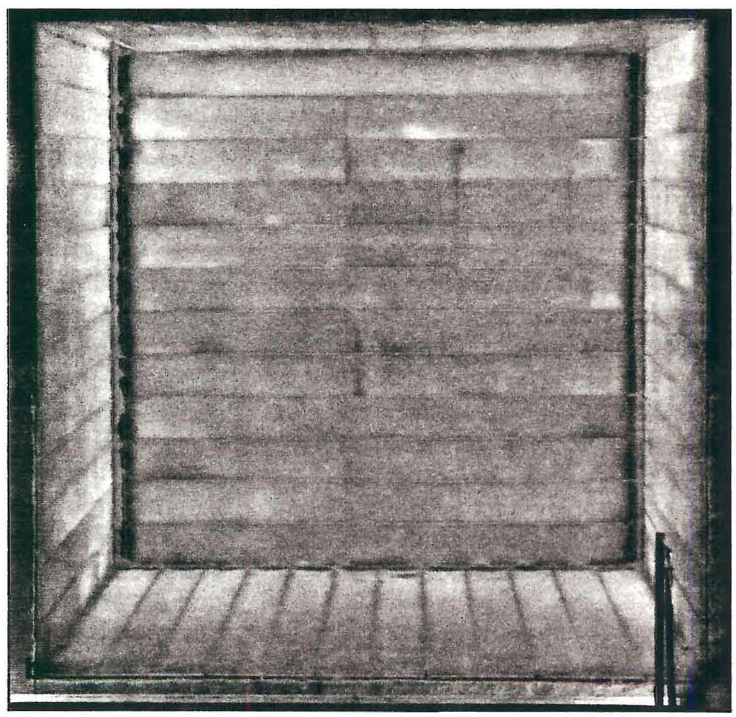

Size of sides:	**2.2 m**
Surface temp:	**800°C**
Natural convection	

Wind velocities in the tunnel range up to 6 m/s and the plate is heated to temperatures as high as 650°C. Depending on the combination of surface temperature and wind velocity, the mode of heat transfer from the vertical plate is either natural convection, mixed convection, or forced convection. In the mixed-convection mode, the boundary-layer flow on the vertical plate is similar to that for mixed convection from an external receiver or a skewed three-dimensional boundary layer, as shown schematically in Figure 4.

Figure 5 shows the domain of new data from this experiment as compared to existing data in the literature in terms of the Grashof number, Gr (a measure of the natural-convection driving force), and the Reynolds number, Re (a measure of the forced-convection driving force) (Box A). Regions dominated by natural, mixed, and forced-convection heat transfer are indicated. The region for which data exist in the literature is shown in dark gray, and is composed mainly of pure natural- and forced-convection data. The unshaded area shows the large region where knowledge has been added to existing information. In addition, there was little information in the literature on the effects of significant fluid property variations at high temperatures on natural-convection or mixed-convection heat transfer for receiver-like geometries. Experiments conducted for conditions on which data already exist, such as low-temperature pure natural convection and pure forced convection, were used as baseline tests to verify the design of the experiment.

We measured both heat transfer from the plate and the boundary-layer profiles of velocity, temperature, and flow angle. The overall or average heat transfer in terms of the Nusselt number (a dimensionless measure of heat transfer—see Box A) is shown in Figure 6 as a function of Reynolds and Grashof numbers. From these heat-transfer measurements we established relationships for mixed convection and high-temperature natural convection. The mixed-convection relationship we developed was one of the experiment's most important findings (Box B).

Our measurements showed an unexpected result in the turbulent mixed-convection boundary layer: the existence of a region of constant flow angle with respect to distance from the wall. This region occurs very near the surface of the plate. We expect that the constant-angle region is a feature of the flow that turbulence models, being developed as a part of detailed efforts to model these types of flows, will need to predict in order to accurately predict heat transfer.

Figure 4.
When air is forced parallel to and horizontally over a heated vertical surface, the air near the surface (the boundary layer) is heated and rises due to buoyancy as it moves downstream. Away from the surface, in the unheated free stream, the flow remains horizontal. This flow pattern results in a skewed three-dimensional boundary layer on the vertical flat plate. Air flow near the wall arcs upward, while air flow in the free stream remains horizontal.

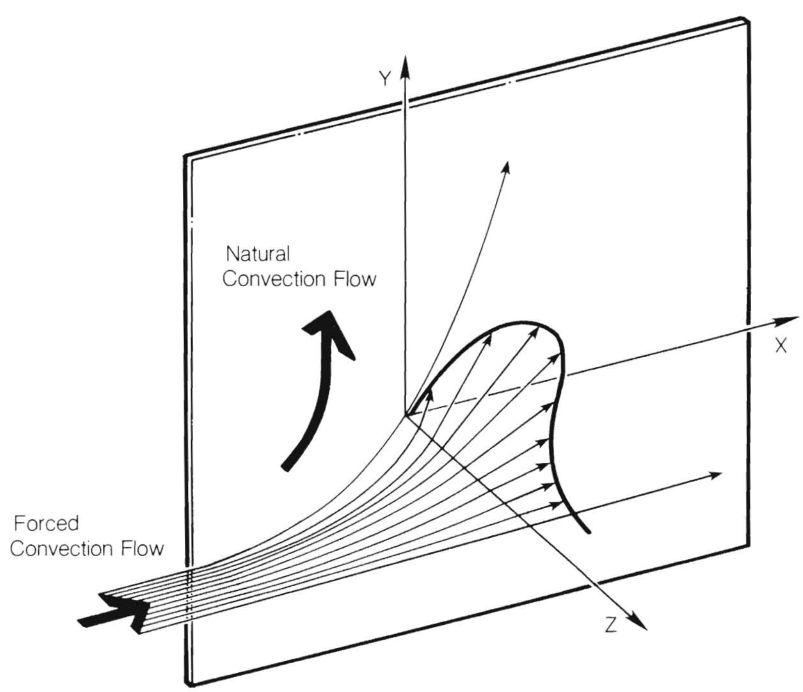

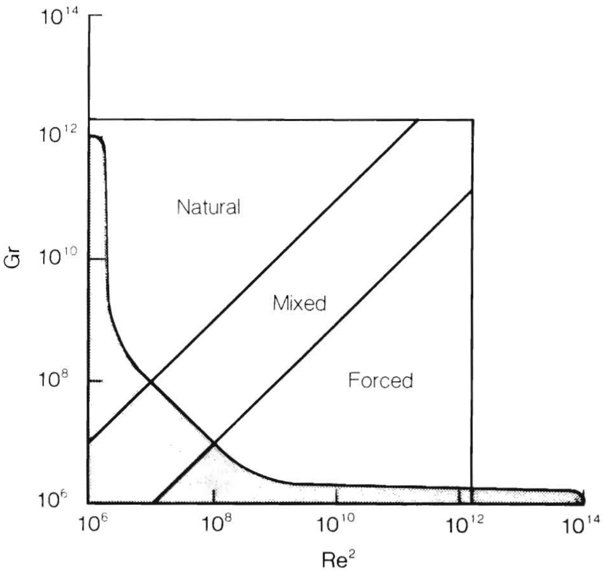

Figure 5.
A significant body of new information on convective heat transfer has been added to the literature (represented by the white region). The Grashof number, Gr, is a measure of the natural-convection driving force, while the Reynolds number, Re, is a measure of the forced-convection driving force. The illustration shows the regions dominated by natural, mixed, and forced convective heat transfer.

Currently, data exist primarily for pure forced convection and low-temperature pure natural convection (dark gray regions). Our experiments provided data for high-temperature turbulent-flow conditions—the first data available for both natural and mixed convection relevant to external receiver geometries.

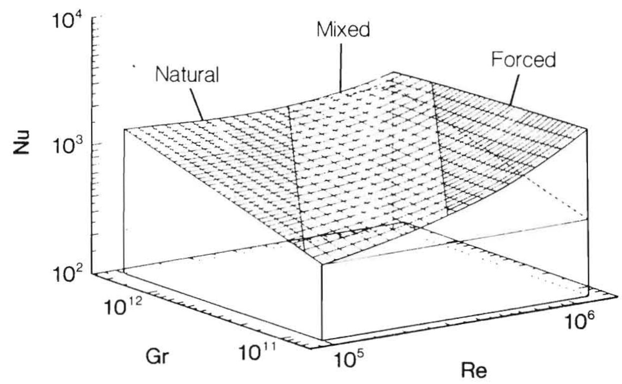

Figure 6.
Experimental heat-transfer data show the conditions for which forced, mixed, and natural convection dominate heat transfer from the test surface. The measured overall or average heat transfer is plotted as the Nusselt number (a dimensionless measure of heat-transfer rate) against the Reynolds and Grashof numbers.

Large Cubical-Cavity Experiment

We designed this experiment (Figures 3b and 7) to produce convective heat-transfer processes similar to those that occur in cavity-type solar central receivers. The cubical geometry was chosen because it is representative of actual receivers and lends itself to theoretical modeling of flow and heat transfer. Interior surfaces were heated electrically as high as 750°C to simulate typical receiver temperatures.

We used two methods to obtain our data: (1) we determined the heat leaving the interior surfaces of the cavity from measured surface temperatures, and (2) we measured velocity, temperature, and radiant-heat flux distributions in the aperture plane to determine the heat leaving the opening in the cavity. As expected, losses from the surfaces were equal to losses through the opening, thus providing a check of the experimental methods.

Air temperature and velocity distributions in the aperture plane (Figure 8) indicate that most of the heat is convected outward from the cavity's top center, with only a fraction escaping at the upper corners. Flow-visualization studies, shown schematically in Figure 8, confirmed this finding.

As shown in Figure 9, flow patterns are caused by air being drawn into the bottom of the cavity, being heated by the surfaces, and rising rapidly to the top of the cavity. The air must then turn and flow horizontally along the cavity ceiling. The air flows from each side wall meet in the middle of the ceiling and, having nowhere else to go, flow downward. Air from the back wall turns along the ceiling and pushes the mass of air near the ceiling out of the cavity.

We added lips to the top and bottom of the opening. While the lips changed the flow pattern, they did not reduce the vigor of the flow or greatly decrease heat transfer.

Remarkably, we found that heat transfer from the large cavity was greater than for natural convection

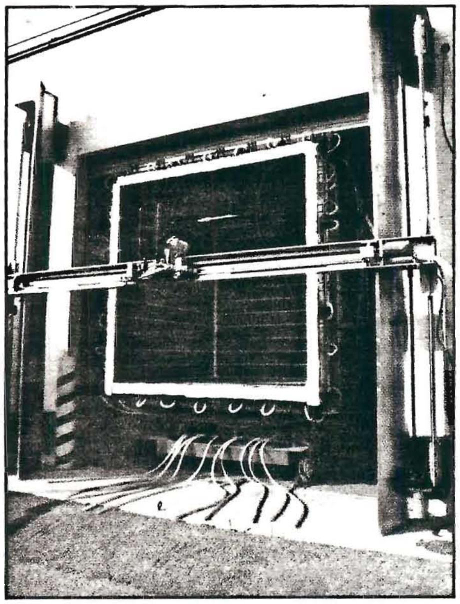

Figure 7.
In the cubical-cavity experiment, the traverse containing thermocouples and other measurement instrumentation is mounted on the exterior building wall. The traverse is a horizontal beam self-cooled by an enclosed water channel on the side facing the cavity. In the back of the beam, sheltered from thermal radiation emitted from the cavity, is a stepping motor that drives the transducer mounting plate in the horizontal direction.

from a flat plate of the same height, total interior surface area, and temperature. This finding is against intuition until it is realized that natural convection inside the cavity enhances heat transfer by impinging on several surfaces in a situation that more nearly resembles mixed convection.

We found that the heat flux—the heat rate per unit area—from the cavity depends only upon the temperature difference between the cavity and ambient air. The consequence is that smaller, less-expensive, scale models of receivers may now be tested with confidence, particularly in cases where the geometry differs greatly from previous experiments.

Box A

Grashof, Reynolds, and Nusselt Numbers

The Grashof number, a dimensionless parameter used in the study of natural convection caused by a hot body, is

$$\mathrm{Gr} = \frac{\alpha \Delta T\, g\, d^3 \rho^2}{\mu^2}$$

where α is the fluid's coefficient of thermal expansion, ΔT is the temperature difference between the hot body and the fluid, g is the acceleration of gravity, d is a characteristic length of the system, ρ is the density of the fluid, and μ is the fluid viscosity. The Grashof number is proportional to the ratio of the buoyant forces caused by heating to the viscous drag on the heated surface.

The Reynolds number, a dimensionless parameter used in the study of forced convection where the effects of viscosity are important, is

$$\mathrm{R} = \frac{\rho\, V\, d}{\mu}$$

where ρ is the density of the fluid, V is its velocity, d is a characteristic length, and μ is the fluid viscosity. The Reynolds number is the ratio of the inertial forces to viscosity.

The Nusselt number, a dimensionless parameter used in the study of forced convection, is

$$\mathrm{Nu} = \frac{\beta\, d}{k}$$

where β is the heat-transfer coefficient, d is a characteristic length of the system, and k is the thermal conductivity of the surrounding fluid. The Nusselt number is the ratio of the convective heat transfer to the conductive heat transfer.

Box B
Calculating Mixed-Convection Heat Transfer

The experiment shows that the average mixed-convection heat transfer, Q_{mixed}, can be estimated by combining two simpler estimates of convective-heat transfer for a problem: one based on the assumption that only forced convection is occurring and the other on the assumption of natural convection for a given problem:

$$Q_{mixed}^{3.2} = Q_{forced}^{3.2} + Q_{natural}^{3.2}$$

This relationship predicts the measured average mixed-convection heat transfer from the vertical plate within a small percentage.

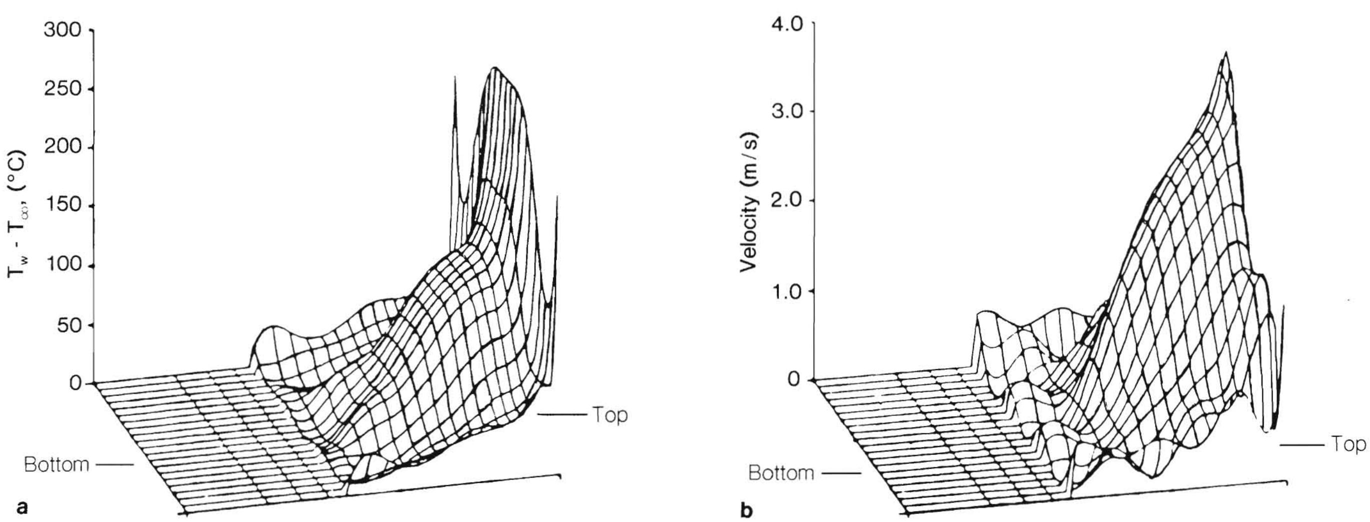

Figure 8.
The temperature difference distribution in the aperture plane (a) shows that the highest temperatures are found in the boundary layer exiting from the top surface of the cavity, with the highest at the center and then the two corners. The orientation of the temperature surface to the cavity aperture is as follows: the left axis is the bottom edge, the right axis (not shown) is the top edge, and the nearly horizontal axes are the sides.

The outflow velocity distribution (b) indicates similar trends. We found inflow velocities to be nearly uniform, in the order of 1.0 m/s, over the lower portion of the cavity. The same characteristics as reported for temperature are apparent here; velocities are greatest in the boundary layer, especially in the center and then the corners. The roughness of the surface near the zero-inflow location is due to fluctuations in the flow and inaccuracies in measuring the low velocities.

Conclusion

Our experiments have given us a better understanding of convective losses from receivers. This new understanding is guiding the development of detailed numerical models for predicting local convective losses, and has allowed us to develop a simplified mathematical model to predict the overall or average convective losses from receivers. This model provides the designer with a practical, easy-to-use tool for estimating the total convective energy loss from a receiver and the uncertainty in that estimate.

For more information, call John Kraabel (415) 422-3408 or Dennis Siebers (415) 422-2078.

(510) 294-2078

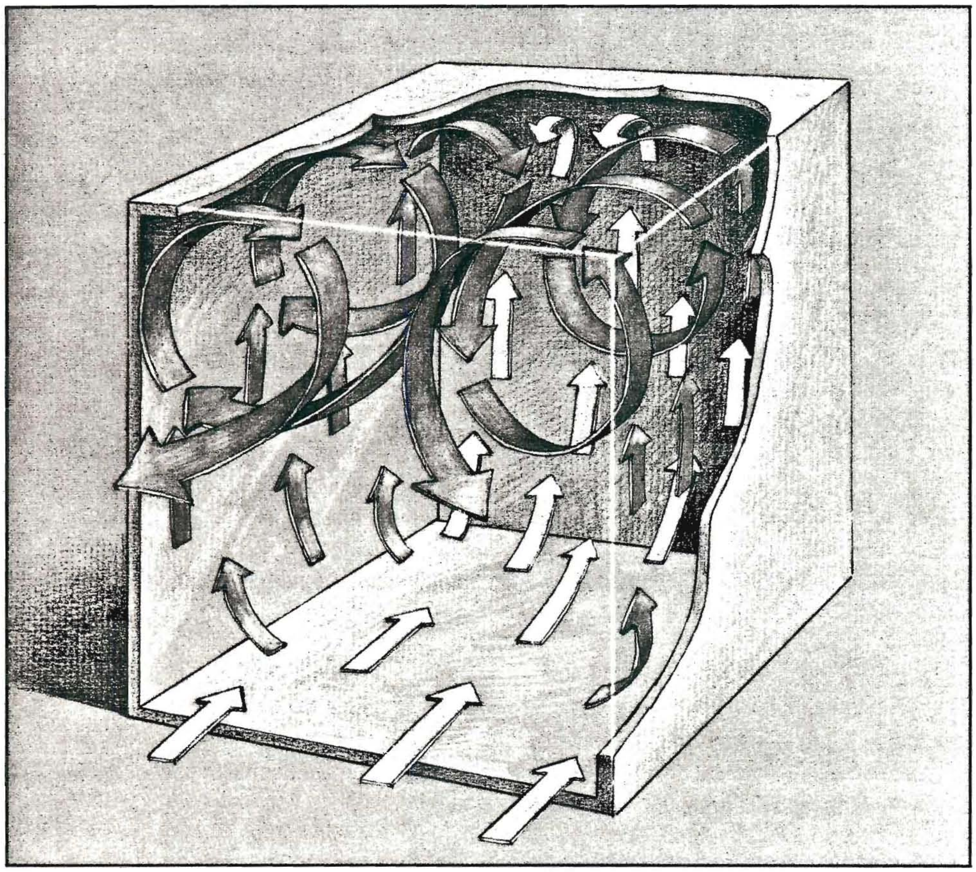

Figure 9.
In a cubical cavity, flow patterns are the result of air being drawn into the bottom of the cavity where it is heated by the surfaces, and then rising rapidly to the top of the cavity. The air must then turn and flow horizontally along the cavity ceiling. Air flowing from each side wall meets in the middle of the ceiling and flows downward. Air from the back wall turns along the ceiling and pushes air out of the cavity.